



Convex Relaxations of the Short-Term Hydrothermal Scheduling Problem

Arild Helseth , *Member, IEEE*, Stefan Jaehnert, and André Luiz Diniz , *Senior Member, IEEE*

Abstract—This paper concerns the assessment of two methods for convex relaxation of the short-term hydrothermal scheduling problem. The problem is originally formulated as a mixed integer programming problem, and then approximated using both Lagrangian and Linear relaxation. The two relaxation methods are quantitatively compared using a realistic data description of the Northern European power system, considering a set of representative days. We find that the Lagrangian relaxation approximates system operational costs in the range 55-81% closer to the mixed integer programming problem solution than the Linear relaxation. We show how these cost gaps vary with season and climatic conditions. Conversely, the differences in both marginal cost of electricity and reserve capacity provided by the Lagrangian and Linear relaxation are muted.

Index Terms—Hydroelectric power generation, integer programming, linear programming, power generation economics.

NOMENCLATURE

Index Sets

$a \in \mathcal{A}$	Set of price areas
$h \in \mathcal{H}$	Set of hydropower reservoirs/stations
$g \in \mathcal{G}$	Set of thermal units
$n \in \mathcal{N}_h$	Set of discharge segments
$m \in \mathcal{M}_g$	Set of generation cost segments
$d \in \mathcal{D}$	Set of price-elastic demands
$c \in \mathcal{C}$	Set of Benders cuts
$k \in \mathcal{K}$	Set of time steps
$j \in \Omega_h^{D/B/S}$	Set of upstream reservoirs discharging (D), bypassing (B) or spilling (S) to h
$\ell \in \mathcal{L}_a^{AC/DC}$	Set of AC or DC lines connected to a .

Parameters

Γ	Conversion between m^3/s and Mm^3
Q_h^D, \bar{Q}_h^D	Bounds on discharge, in m^3/s
\bar{Q}_{hn}^D	Upper discharge bound for segment n , in m^3/s

Manuscript received June 4, 2020; revised September 28, 2020 and November 18, 2020; accepted December 19, 2020. Date of publication December 24, 2020; date of current version June 18, 2021. This work was supported by the Research Council of Norway Project 268014. Paper no. TPWRS-00 929-2020. (Corresponding author: Arild Helseth.)

Arild Helseth and Stefan Jaehnert are with the Energy Systems, SINTEF Energy Research, Trondheim 7491, Norway (e-mail: arild.helseth@sintef.no; stefan.jaehnert@sintef.no).

André Luiz Diniz is with the DEA - Optimization and Environmental Department, CEPEL, Brazilian Electric Energy Research Center, Rio de Janeiro 22220-040, Brazil (e-mail: diniz@cepel.br).

Color versions of one or more figures in this article are available at <https://doi.org/10.1109/TPWRS.2020.3047346>.

Digital Object Identifier 10.1109/TPWRS.2020.3047346

Q_h^B, \bar{Q}_h^B	Bounds on bypass for station h , in m^3/s
V_h, \bar{V}_h	Bounds on volume for reservoir h , in Mm^3
P_h, \bar{P}_h	Bounds on generation for station h , in MW
P_g, \bar{P}_g	Bounds on generation for unit g , in MW
\bar{P}_{gm}	Upper bound on thermal generation for unit g and segment m , in MW
$\Delta_{Q_h^D}$	Max. ramping on discharge, in $\text{m}^3/\text{s}/\text{h}$
Δ_{P_g}	Max. ramping on generation, in MW/h
Δ_{F_ℓ}	Max. ramping on HVDC cable ℓ , in MW/h
C_{0g}^G	No-load cost for unit g , in €
C_g^G, C_{mg}^G	Marginal cost for unit g , in €/MWh
C_g^{SU}, C_h^{SU}	Start-up cost of units and stations, in €
C_g^{SD}, C_h^{SD}	Shut-down cost of units and stations, in €
C_a^R	Cost of curtailment in area a , in €/MWh
C_{dk}^D	Marginal value of demand, in €/MWh
I_{hk}	Inflow to reservoir h , in Mm^3
D, D_{ak}	Price inelastic demand (in area a), in MW
$R_a^{F+/-}$	Spinning up/down-regulation reserve requirement in area a , in MW
R_a^{S+}	Non-spinning up-regulation reserve requirement in area a , in MW
W_{ak}	Wind power in area a , in MW
η_{hn}, η_{hN}	Energy equivalent for station h , discharge segment n or $N= \mathcal{N} $, in $\text{MW}/\text{m}^3/\text{s}$
π_{hc}	Coefficient for Benders cut c , in €/Mm ³
β_c	Right-hand side for Benders cut c , in €
$\gamma_{a\ell}$	Direction of line ℓ , seen from area a , $\{-1, 1\}$
$\Phi_{a\ell}$	PTDF from area a on line ℓ
F_ℓ	Max. flow on line ℓ , in MW
$\hat{\lambda}_{ak}^{i,*}$	Lagrangian multiplier, where * reflects subscripts $P, F+, F-, S+$, in €/MWh
$\hat{\lambda}_c^{i,C}$	Lagrangian multiplier for cut c , fraction
g^i	Mismatches in relaxed constraints, in MW
tol_ϵ, tol_G	Convergence tolerance used in Lagrangian relaxation.

Decision Variables

α	Future expected cost, in €
v_{hk}, v_{hK}	Reservoir vol., step k or $K = \mathcal{K} $, in Mm^3
q_{hk}^D	Discharge allocated station, in m^3/s
q_{hnk}^D	Discharge through segment n , in m^3/s
q_{hk}^B	Bypass passing station, in m^3/s
q_{hk}^S	Spillage from reservoir, in m^3/s
$r_{hk}^{F+/-}$	Spinning up/down-regulating reserves, in MW
$r_{h/g,k}^{S+}$	Non-Spinning up-regulating reserves, in MW

$c_{gk}^{SU/SD}$	Start-up/shut-down cost of unit, in €
$c_{hk}^{SU/SD}$	Start-up/shut-down cost of stations, in €
$u_{h/g,k}$	Commitment status of station/unit, binary
$p_{h/g,k}$	Generation from station/unit, in MW
p_{ak}^{inj}	Net injection of power in area a , in MW
p_{gmk}	Generation on unit segment m , in MW
y_{dk}^D	Price-elastic demand, in MW
y_{ak}^R	Curtailed power in area a , in MW
$f_{\ell k}$	Flow on line ℓ , in MW
$f_{abk}^{F+/-}$	Reserved line capacity for spinning and up/down-regulating reserves, in MW
f_{abk}^{S+}	Reserved line capacity for non-spinning and up-regulating reserves, in MW
z_{ak}^*	Auxiliary variables, where $*$ reflects subscripts $P, F+, F-, S+$, in MW
λ_{ak}^*	Lagrangian multiplier, where $*$ reflects subscripts $P, F+, F-, S+$, in €/MWh
λ_c^C	Lagrangian multiplier for cut c , fraction.

I. INTRODUCTION

THE use of fundamental optimization and simulation models for forecasting system operational costs and the marginal costs of electricity (MCE) is a well-established practice in many power markets [1], [2]. A primary challenge in the use of fundamental models for systems with high shares of hydropower is to find the marginal value of water. Due to the long-term reservoir storage constraints and uncertainty in inflows, the marginal value of water is found by solving the long-term hydrothermal scheduling problem, covering a sufficiently long time period and with an appropriate representation of uncertainties. Such long-term models are widely used for forecasting operational costs and MCE in hydropower-dominated systems [3], [4].

Short-term hydrothermal scheduling (STHTS) models typically have a time-horizon of a few weeks or shorter, with targets or strategies for reservoir operation obtained from the longer-term models. This allows the representation of more details, such as exact unit commitment, and nonconvex hydropower generation functions [5], [6]. Although the level of details provided in the short-term scheduling is needed to provide realistic operational schedules, such details are often neglected in the longer-term models to reduce the computational effort. Thus, there is an inconsistency in system representation between the long-term models used for operational cost and MCE forecasting and the short-term models used for operational scheduling [7].

In this work, we study the STHTS as a part of the long-term scheduling for a case study of the Northern European power system. The emphasis is on computing the system operational costs, the MCE and the marginal costs of different types of reserve capacity (MCR). We formulate the STHTS optimization problem as a mixed integer programming problem (MIP) to obtain detailed cost and marginal cost estimates. Solving the MIP problem is computationally demanding. It also complicates the process of computing MCE and MCR, since the dual variables associated with the supply-demand constraints are not available. Thus, we solve two different convex relaxations of the STHTS

problem and compare their solutions and computation times to those of the MIP problem.

By adding STHTS results for selected representative days, the aim is to enhance the forecasts of operational costs, MCE and MCR from long-term models, which in turn leads to better and more robust investment decisions.

A. Literature Review

Pricing in centrally-dispatched pool markets with nonconvexities is thoroughly discussed in the literature, see e.g. [8]–[16], and has similarities to our above-stated problem. In contrast to these works, we are concerned with costs and marginal costs, and not prices within a specific market context.

Two convex relaxation methods of the pricing problem have been intensively studied, namely the Convex Hull (CH) and the Linear Relaxation (LIR) method. The CH method finds the convex envelope of the system cost function and thus a lower bound on the minimum operational cost. The gradients of this convex envelope are known as CH prices [8], and these can be obtained by applying Lagrangian Relaxation (LR) (or Benders decomposition, as recently proposed in [17]) to the market clearing problem. In the LIR method all integer variables are relaxed to continuous variables before solving the relaxed LP problem to obtain dual values (prices). Thus, the LIR method will at best provide a convex relaxation as tight as the CH. In [12] the authors find that a variant of the LIR method (primal convex relaxation) suffices to find the exact CH prices for a market clearing problem with ancillary services. Moreover, the work in [13] identifies conditions where the LIR prices can provide exact approximations to CH prices. However, both [12], [13] point out that the presence of ramping constraints challenge the tightness of the relaxations. To this end, a substantial amount of research has focused on tightening the ramping-constrained thermal unit commitment problem, as thoroughly reviewed in [18], and detailed in recent studies such as [19], [20].

The STHTS problem has been extensively investigated by researchers for decades, see e.g. the recent reviews in [5], [21] and references therein. From a mathematical point of view, the problem can be characterized as a combinatorial, nonlinear and nonconvex. In addition to the unit commitment decisions of generating units, the hydropower production function is typically a major contributor to nonconvexities in the STHTS formulation. In [22] the convex hull of this function was found a priori and expressed by hyperplanes. Approaches to convexify the hydropower production function within the long-term models are presented in [23]–[25]. Other examples of nonconvexities are due to irrigation [26] and river level and river-routing constraints [27].

Realistic instances of the STHTS soon become large-scale optimization problems, which can be solved efficiently by decomposition. One of the most applied techniques for solving large-scale STHTS problems is LR, where the original problem is divided into subproblems, enabling a distributed solution approach. Several successful applications of LR to the STHTS problem have been reported in the literature, such as [28]–[34]. Unlike these works, which primarily emphasize on the primal

TABLE I
EXAMPLE DATA

	Unit A	Unit B
Start-up cost [€]	0	6000
Var. cost seg. 1 [€/MWh]	65	40
Var. cost seg. 2 [€/MWh]	110	90

solution, we will study properties of the dual solution, i.e., lower cost bounds and marginal costs, in this work.

B. Contributions

The major novel contribution in this work lies in the quantitative assessment of the differences in operational costs, MCE and MCR obtained by the LIR and LR convex relaxation methods when solving realistic and large-scale¹ instances of the STHTS problem. The problem at hand couples multiple time steps and has multiple types of ramping constraints, challenging the tightness of the LIR. While authors in [12], [13] demonstrated that the solutions from the LIR and LR methods coincide in the absence of ramping constraints for thermal-based systems, we quantify how the solutions from the two relaxation methods differ in the presence of ramping constraints in a system with a large share of hydropower. Moreover, we identify how the approximation errors in operational costs systematically vary with seasons and climatic conditions when using the LIR method compared to the tighter LR method and to the exact MIP problem formulation. To the best of the authors knowledge, similar quantitative assessments have not been carried out for large-scale hydro-dominated systems before.

The proposed LR solution technique is inspired by [32]–[34], with duplicate variables for representing the generation per technology and per price area. The STHTS problem is decomposed into separate hydropower and thermal unit commitment problems, coordinated through updated prices, as described in Section IV. Different from [33] we split Benders cuts approximating the future expected cost function into parts that can be embedded in the hydropower subproblems, avoiding additional duplicate variables per reservoir. This proved to be computationally more efficient for the large-scale system being studied.

II. ILLUSTRATIVE EXAMPLE

The following two examples serve to illustrate the basic properties of the two relaxation methods considered in this work. System data are obtained from [8]. Two thermal power units (named A and B) serve a demand. Both units have a cost curve comprising two variable cost segments, each with a capacity (\bar{P}_{gm}) of 100 MW, and unit B also has a start-up cost, as shown in Table I. Note that the piecewise linear part of the cost curve assumes that cost segments are loaded according to increasing cost coefficients, and that no binary variables are needed to assure correct loading of segments. This assumption is also made when modeling thermal units in Section III.

¹The case study considers a data description of the Northern European power system, comprising 549 hydropower stations and 252 thermal units exceeding 10 MW installed capacity.

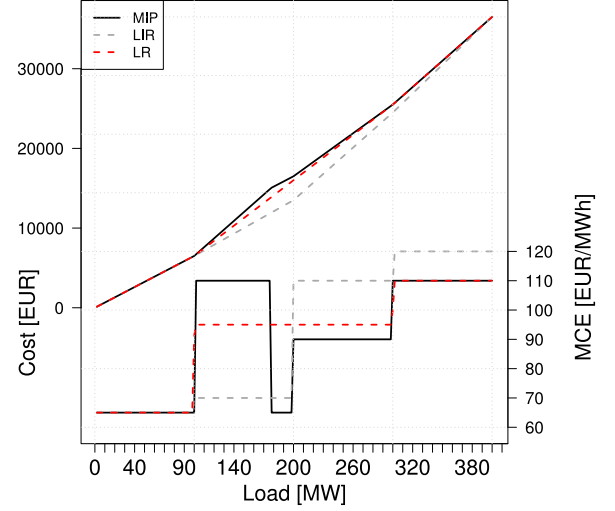


Fig. 1. Costs and MCE for the single-period example.

A. Single Period

To find the optimal dispatch for a single hour with a predefined demand, we formulate the problem as follows:

$$\min \sum_{g \in \mathcal{G}} \sum_{m \in \mathcal{M}_g} \left(C_{gm}^G p_{gm} + C_g^{SU} u_g \right) \quad (1a)$$

$$p_g = \sum_{m \in \mathcal{M}_g} p_{gm} \quad \forall g \quad (1b)$$

$$\sum_{g \in \mathcal{G}} p_g \geq D \quad (1c)$$

$$p_g \leq u_g \bar{P}_g \quad \forall g \quad (1d)$$

$$p_{gm} \leq \bar{P}_{gm} \quad \forall g, m \quad (1e)$$

$$u_g \in \{0, 1\} \quad \forall g \quad (1f)$$

We let the demand vary from 0 to 400 MW, and obtain the minimum operating costs and the corresponding MCE in Fig. 1. The results stem from solving problem (1) in three different ways:

- 1) As an MIP problem (denoted MIP). Once the optimal commitments (u_g) are found, these variables are fixed and the corresponding LP problem is solved to obtain the MCE, as the dual value of (1c).
- 2) Relax (1c) and solve the decomposed problem using LR (denoted LR). The MCE equals the optimal Lagrangian multiplier for each value of demand.
- 3) Relax (1f) by letting $u_g \in [0, 1]$ so that (1) can be solved as an LP (denoted LIR). The MCE equals the dual value of (1c).

From Fig. 1 we observe that MCE obtained using the MIP approach sometimes decreases with higher demand, since the commitment is done prior to computing the MCE. For the LR and LIR methods, the MCE will always increase with increasing demand. The LR solution provides the convex envelope of the MIP cost function, whereas the LIR underestimates the

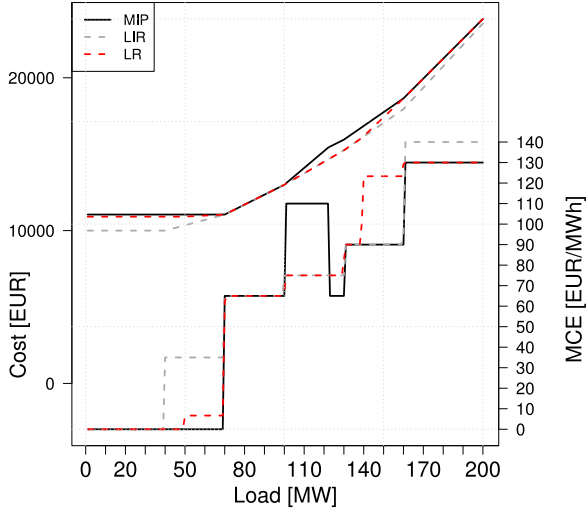


Fig. 2. Costs and first-period MCE for the two-period example.

convex cost envelope at demands higher than 100 MW. These results are in line with [8]. We emphasize that MCE computed by the LIR and LR approaches have different properties than those computed by the MIP approach, since the LIR and LR do include the fixed cost elements (start-up cost in this case) while MIP does not. The implications of using MCE based on different approaches (or ‘pricing rules’) for investment signals is discussed in [35], [36], but are not further discussed in this work.

Slightly reformulating the problem, replacing (1b)–(1e) by (2a)–(2b) serves to tighten the problem formulation, and the cost and MCE curves for LR and LIR in Fig. 1 will coincide. Note that the MIP and LR solutions are not affected by the reformulation. This exemplifies the findings in [13], where the LIR method was proven to provide exact approximations to the CH pricing with careful modeling.

$$\sum_{g \in \mathcal{G}} \sum_{m \in \mathcal{M}_g} p_{gm} \geq D \quad (2a)$$

$$p_{gm} \leq u_g \bar{P}_{gm} \quad \forall g, m \quad (2b)$$

B. Two-Period

Next we extend the example above to cover two time periods of one hour each. The maximum ramping is limited to ± 30 MW/h for each of the units. The mathematical model is shown in (3). We fix the demand in the second period to 100 MW and let the demand in the first period vary from 0 to 200 MW. The minimum operating cost and the corresponding MCE for the first period are shown in Fig. 2.

$$\min \sum_{k \in \mathcal{K}} \sum_{g \in \mathcal{G}} \sum_{m \in \mathcal{M}_g} (C_{gm}^G p_{gmk} + C_g^{SU} u_{gk}) \quad (3a)$$

$$\sum_{g \in \mathcal{G}} \sum_{m \in \mathcal{M}_g} p_{gmk} \geq D_k \quad \forall k \quad (3b)$$

$$p_{gmk} \leq u_{gk} \bar{P}_{gm} \quad \forall g, m, k \quad (3c)$$

$$-\Delta P_g \leq \sum_{m \in \mathcal{M}_g} p_{gmk} - \sum_{m \in \mathcal{M}_g} p_{gm, k-1} \leq \Delta P_g, \quad \forall g, k = 2 \quad (3d)$$

$$u_{gk} \in \{0, 1\} \quad \forall g, k \quad (3e)$$

The presence of ramping limits between the two periods contributes to underestimating the convex cost envelope when applying LIR. As proved in [37], a complete linear description of the convex envelope can be defined for the general two-period unit commitment problem with ramping constraints. In our example, it is sufficient to tighten (3d) by introducing $u_{g, k-1}$ and u_{gk} as shown in (4), to ensure that costs and MCE obtained by the LIR and LR methods coincide.

$$-\Delta P_g u_{g, k-1} \leq \sum_{m \in \mathcal{M}_g} p_{gmk} - \sum_{m \in \mathcal{M}_g} p_{gm, k-1} \leq \Delta P_g u_{gk}, \quad \forall g, k = 2 \quad (4)$$

The MIP and LR solutions do not change with this reformulation. For more realistic systems, with many types of ramping and other time-coupling constraints covering multiple time steps, a cost gap between the LR and LIR methods seems to be inevitable.

III. PROBLEM FORMULATION

In the following we formulate the STHTS optimization problem, which is solved for a specific day to obtain operating costs and marginal costs of electricity and different types of reserve capacity. The model is formulated as a deterministic MIP problem. For the ease of formulation, but without loss of generality, the length of each time step is assumed to be one hour.

A. Objective Function

$$\begin{aligned} \min \sum_{k \in \mathcal{K}} \left[\sum_{h \in \mathcal{H}} (c_{hk}^{SU} + c_{hk}^{SD}) + \sum_{g \in \mathcal{G}} (c_{gk}^{SU} + c_{gk}^{SD}) \right. \\ \left. + \sum_{g \in \mathcal{G}} (C_{0g}^G u_{gk} + \sum_{m \in \mathcal{M}_g} C_{mg}^G p_{mgk}) \right. \\ \left. + \sum_{a \in \mathcal{A}} C_a^R y_{ak}^R - \sum_{d \in \mathcal{D}} C_{dk}^D y_{dk}^D \right] + \alpha \quad (5) \end{aligned}$$

The objective (5) is to minimize the system costs associated with operation of the system in the current decision period and the expected cost of operating the system in the future. The current cost has three contributions: Costs for starting and stopping hydro and thermal generators, according to (6m)–(6n) and (7d)–(7e); The no-load and variable cost of thermal generation; and the curtailment of price-inelastic demand. Meeting the price-elastic demand can be seen as a revenue. The future expected operating cost (α) is constrained by Benders cuts in (8d), which in this work was obtained from the long-term hydrothermal scheduling model described in [3]. Note that α

reflects the expected cost of operation for stages beyond the short-term horizon represented here, and that it depends on the system state at the end of the short-term horizon.

B. Hydropower Constraints

$$v_{hk} + \Gamma \left(q_{hk}^D + q_{hk}^B + q_{hk}^S \right) - \Gamma \left(\sum_{j \in \Omega_h^D} q_{jk}^D + \sum_{j \in \Omega_h^B} q_{jk}^B + \sum_{j \in \Omega_h^S} q_{jk}^S \right) - v_{h,k-1} = I_{hk} \quad \forall h, k \quad (6a)$$

$$\underline{Q}_h^D \leq q_{hk}^D \leq \overline{Q}_h^D \quad \forall h, k \quad (6b)$$

$$\underline{Q}_h^B \leq q_{hk}^B \leq \overline{Q}_h^B \quad \forall h, k \quad (6c)$$

$$\underline{V}_h \leq v_{kh} - \frac{\Gamma}{\eta_{hN}} (r_{hk}^{F+} + r_{hk}^{S+}) \quad \forall h, k \quad (6d)$$

$$v_{kh} + \frac{\Gamma}{\eta_{hN}} r_{hk}^{F-} \leq \overline{V}_h \quad \forall h, k \quad (6e)$$

$$-\Delta_{Q_h^D} u_{h,k-1} \leq q_{hk}^D - q_{h,k-1}^D \leq \Delta_{Q_h^D} u_{hk} \quad \forall h, k \quad (6f)$$

$$p_{hk} = \underline{P}_h u_{hk} + \sum_{n \in \mathcal{N}_h} \eta_{hn} q_{nhk}^D \quad \forall h, k \quad (6g)$$

$$q_{hk}^D = \underline{Q}_h^D u_{hk} + \sum_{n \in \mathcal{N}_h} q_{nhk}^D \quad \forall h, k \quad (6h)$$

$$0 \leq q_{nhk}^D \leq \overline{Q}_{nhk}^D u_{hk} \quad \forall n, h, k \quad (6i)$$

$$p_{hk} + r_{hk}^{F+} \leq \overline{P}_h u_{hk} \quad \forall h, k \quad (6j)$$

$$p_{hk} + r_{hk}^{F+} + r_{hk}^{S+} \leq \overline{P}_h \quad \forall h, k \quad (6k)$$

$$\underline{P}_h u_{hk} \leq p_{hk} - r_{hk}^{F-} \quad \forall h, k \quad (6l)$$

$$c_{hk}^{SU} \geq C_h^{SU} (u_{hk} - u_{h,k-1}) \quad \forall h, k \quad (6m)$$

$$c_{hk}^{SD} \geq C_h^{SD} (u_{h,k-1} - u_{h,k}) \quad \forall h, k \quad (6n)$$

The hydropower system is modeled using the building blocks of hydropower *modules* h connected through the three waterways discharge, bypass and spillage. A module comprises one reservoir and one power station, and has a set of upstream modules Ω_h from which it receives water through one or more of the waterways. Constraints (6a) balance the content in each reservoir. The discharge (6b), bypass (6c) and reservoir (6d)–(6e) variables are often subject to seasonal constraints to ensure that watercourses are operated in a sustainable manner. In (6d) we require that there is sufficient water left in the reservoir to serve activation of procured up-regulating reserves, whereas (6e) requires sufficient storage capacity left to down-regulate hydropower generation without spilling water. Some rivers have environmental constraints as in (6f), limiting the changes in discharge (can also be on bypass) between time steps. Pumps and pumped-storage power plants are not included in the formulation above for brevity. Note also the simplification made by neglecting water travel times in the model formulation. These are generally not important for most parts of the Nordic system.

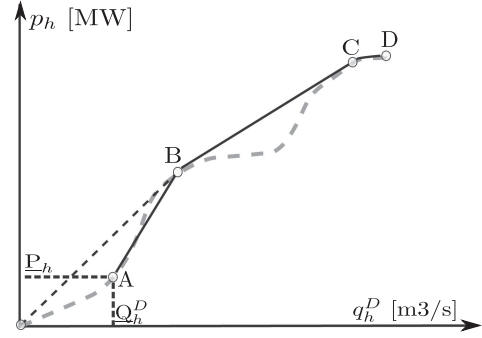


Fig. 3. PQ-curve modeling.

In practice a hydropower station comprises many units (or aggregates), and for fine precisions in the calculations, the individual units should be represented, as detailed in [5]. For the large-scale system considered here with more than 1000 modules, a unit-based approach was not possible. This is primarily due to lack of detailed data, but also due to the significant increase in computational complexity. An approximate curve representing the power output as a function of station discharge (PQ curve) is presented instead, as explained in the following. A station with several units will have a best efficiency point for each combination of units. This is illustrated in Fig. 3 where the output from two units loaded in sequence is shown as the grey-dotted line with best efficiency points B and C. A linear approximation of the PQ-curve in Fig. 3 uses the points B, C and D, which is a good approximation when the units are operated at their best efficiency points B and C. However, if the station has to run on low output, e.g., close to point A, to deliver down-regulation reserves or to meet a minimum discharge requirement, the discharge is underestimated or the power output is overestimated with the linear approach, respectively. To reflect this, we introduce a minimum discharge (\underline{Q}_h^D) and power output (\underline{P}_h) and model the station's power output as in (6g)–(6i). This corresponds to the curve defined by the points A, B, C and D. The PQ-curve is scaled according to the actual head at the beginning of the day. This is a simplification, assuming that the relative head will vary little during the day, which is typically the case for the many high-head stations in Norway. Equations (6j)–(6l) determine the maximum and minimum power output depending on the commitment status and the delivery of fast and slow reserves.

C. Thermal Constraints

The cost of operating thermal generation units in (5) comprises fixed and variable components. The variable component consists of a piecewise linear cost curve, with costs coefficients C_{gm}^G increasing with increasing m . The generation is expressed in (7a), and generation segments are bounded in (7b). The ability to provide non-spinning up-regulation reserves is formulated in (7c), and the start-up and shut-down costs in (7d)–(7e), respectively.

$$p_{gk} = \underline{P}_g u_{gk} + \sum_{m \in \mathcal{M}_g} p_{mgk} \quad \forall g, k \quad (7a)$$

$$p_{mgk} \leq \overline{P}_{mgk} u_{gk} \quad \forall m, g, k \quad (7b)$$

$$p_{gk} + r_{gk}^{S+} \leq \bar{P}_g u_{gk} \quad \forall g, k \quad (7c)$$

$$c_{gk}^{SU} \geq C_g^{SU} (u_{gk} - u_{g,k-1}) \quad \forall g, k \quad (7d)$$

$$c_{gk}^{SD} \geq C_g^{SD} (u_{g,k-1} - u_{g,k}) \quad \forall g, k \quad (7e)$$

In addition to (7), ramp-up and ramp-down limits, start-up and shut-down ramp limits and minimum up and down-time constraints were modeled following the equations (16)–(26) in [38] (Section II B). We do not explicitly state these equations here for brevity. The formulation in [38] uses one binary variable per thermal generation unit, and is proven to be computationally efficient.

D. System-Wide Constraints

$$\sum_{g \in \mathcal{G}_a} p_{gk} + \sum_{h \in \mathcal{H}_a} p_{hk} - \sum_{d \in \mathcal{D}_a} y_{dk}^D + y_{ak}^R - \sum_{\ell \in \mathcal{L}^{AC}} \gamma_{a\ell} f_{\ell k} - \sum_{\ell \in \mathcal{L}^{DC}} \gamma_{a\ell} f_{\ell k} = D_{ak} - W_{ak} \quad \forall a, k \quad (8a)$$

$$f_{\ell k} = \sum_{a \in \mathcal{A}} \Phi_{a\ell} p_{ak}^{inj} \quad \forall \ell \in \mathcal{L}^{AC}, k \quad (8b)$$

$$-\Delta F_{\ell} \leq f_{\ell k} - f_{\ell, k-1} \leq \Delta F_{\ell} \quad \forall \ell \in \mathcal{L}^{DC}, k \quad (8c)$$

$$\alpha + \sum_{h \in \mathcal{H}} \pi_{hc} v_{hk} \geq \beta_c \quad k = |\mathcal{K}|, \forall c \in \mathcal{C} \quad (8d)$$

$$\sum_{h \in \mathcal{H}_a} r_{hk}^{F+} + \sum_{\substack{\ell: (a,b) \\ \in \mathcal{L}^{AC}}} (f_{bak}^{F+} - f_{abk}^{F+}) \geq R_a^{F+} \quad \forall a, k \quad (8e)$$

$$\sum_{h \in \mathcal{H}_a} r_{hk}^{F-} + \sum_{\substack{\ell: (a,b) \\ \in \mathcal{L}^{AC}}} (f_{bak}^{F-} - f_{abk}^{F-}) \geq R_a^{F-} \quad \forall a, k \quad (8f)$$

$$\sum_{h \in \mathcal{H}_a} r_{hk}^{S+} + \sum_{g \in \mathcal{G}_a} r_{gk}^{S+} - \sum_{\ell: (a,b) \in \mathcal{L}^{AC}} (f_{bak}^{S+} - f_{abk}^{S+}) \geq R_a^{S+} \quad \forall a, k \quad (8g)$$

$$f_{\ell k} + f_{abk}^{F+} + f_{abk}^{S+} \leq F_{\ell} \quad \forall \ell \in \mathcal{L}^{AC}, k \quad (8h)$$

$$-F_{\ell} \leq f_{\ell k} - f_{bak}^{F+} - f_{bak}^{S+} \quad \forall \ell \in \mathcal{L}^{AC}, k \quad (8i)$$

$$f_{\ell k} + f_{bak}^{F-} \leq F_{\ell} \quad \forall \ell \in \mathcal{L}^{AC}, k \quad (8j)$$

$$-F_{\ell} \leq f_{\ell k} - f_{abk}^{F-} \quad \forall \ell \in \mathcal{L}^{AC}, k \quad (8k)$$

$$0 \leq f_{abk}^{F+/-}, f_{bak}^{F+/-}, f_{abk}^{S+}, f_{bak}^{S+} \leq \Psi F_{\ell} \quad \forall \ell \in \mathcal{L}^{AC}, k \quad (8l)$$

$$0 \leq f_{abk}, f_{bak} \leq F_{\ell} \quad \forall \ell \in \mathcal{L}^{DC}, k \quad (8m)$$

Power balances for each price area in each time step are provided in (8a). Exchange with neighboring price areas is facilitated through a combination of AC lines and HVDC cables. A grid equivalent, represented by a power transfer distribution (PTDF) matrix, allows linearized (or ‘DC’) power flow in (8b) representing the AC lines. In (8b), p_{ak}^{inj} represents the net power injection in a price area, including all elements in (8a) except

from the flow in the AC grid. Flow in HVDC cables are constrained by the maximum capacities in (8m) and ramping limits in (8c). The future expected operating cost (α) is constrained by Benders cuts in (8d).

Both up- and down-regulating spinning reserves can be allocated to individual hydropower stations to meet the demand in (8e) and (8f), respectively. Non-spinning up-regulating reserves can be allocated to both hydro stations and thermal units in (8g). Moreover, we allow reserves to be exchanged through AC transmission lines in (8h)–(8l), at a maximum fraction Ψ of the line capacity.

IV. LAGRANGIAN RELAXATION

We apply LR to decompose the MIP problem defined by (5)–(8), building further on the concept of variable splitting presented in [32]–[34].

A. Decomposition

The system-wide constraints in (8) express functional relationships between decisions variables in several price areas. In the LR approach we relax these system-wide constraints. First, a set of auxiliary variables z^P , z^{F+} , z^{F-} and z^{S+} per price area and time step are introduced in (9), with the Lagrangian multipliers in parenthesis:

$$z_{ak}^P - \sum_{h \in \mathcal{H}_a} p_{hk} - \sum_{g \in \mathcal{G}_a} p_{gk} = 0 \quad (\lambda_{ak}^P) \quad (9a)$$

$$z_{ak}^{F+} - \sum_{h \in \mathcal{H}_a} r_{hk}^{F+} = 0 \quad (\lambda_{ak}^{F+}) \quad (9b)$$

$$z_{ak}^{F-} - \sum_{h \in \mathcal{H}_a} r_{hk}^{F-} = 0 \quad (\lambda_{ak}^{F-}) \quad (9c)$$

$$z_{ak}^{S+} - \sum_{h \in \mathcal{H}_a} r_{hk}^{S+} - \sum_{g \in \mathcal{G}_a} r_{gk}^{S+} = 0 \quad (\lambda_{ak}^{S+}) \quad (9d)$$

The constraints in (9) are relaxed and the Lagrangian function can be expressed as:

$$\begin{aligned} \mathcal{L}(x, \lambda) = & (5) + \sum_{a \in \mathcal{A}} \sum_{k \in \mathcal{K}} \left(\lambda_{ak}^P \left(z_{ak}^P - \sum_{h \in \mathcal{H}_a} p_{hk} - \sum_{g \in \mathcal{G}_a} p_{gk} \right) \right. \\ & + \lambda_{ak}^{F+} \left(z_{ak}^{F+} - \sum_{h \in \mathcal{H}_a} r_{hk}^{F+} \right) + \lambda_{ak}^{F-} \left(z_{ak}^{F-} - \sum_{h \in \mathcal{H}_a} r_{hk}^{F-} \right) \\ & \left. + \lambda_{ak}^{S+} \left(z_{ak}^{S+} - \sum_{h \in \mathcal{H}_a} r_{hk}^{S+} - \sum_{g \in \mathcal{G}_a} r_{gk}^{S+} \right) \right) \\ & + \sum_{c \in \mathcal{C}'} \lambda_c^C \left(\beta_c - \alpha - \sum_{h \in \mathcal{H}} \pi_{hc} v_{hk} \right) \end{aligned} \quad (10)$$

The relaxation of (9) facilitates a decomposable problem structure, giving separate multi-period MIP subproblems for the hydropower (11) and thermal (12) unit commitment per price area, while keeping the remaining cost components and

constraints in a “market” problem in (13).

$$Z_a^H = \max \sum_{k \in \mathcal{K}} \sum_{h \in \mathcal{H}_a} \left(\hat{\lambda}_{ak}^{i,P} p_{hk} + \hat{\lambda}_{ak}^{i,F+} r_{hk}^{F+} + \hat{\lambda}_{ak}^{i,F-} r_{hk}^{F-} + \hat{\lambda}_{ak}^{i,S+} r_{hk}^{S+} - c_{hk}^{SU} - c_{hk}^{SD} \right) + \sum_{c \in \mathcal{C}'} \hat{\lambda}_c^{i,C} \sum_{h \in \mathcal{H}_a} \pi_{hc} v_{hK} \quad (11)$$

s.t: (6).

$$Z_a^G = \max \sum_{k \in \mathcal{K}} \sum_{g \in \mathcal{G}_a} \left(\hat{\lambda}_{ak}^{i,P} p_{gk} + \hat{\lambda}_{ak}^{i,S+} r_{gk}^{S+} - C_{0g}^G u_{gk} - \sum_{m \in \mathcal{M}_g} C_{mg}^G p_{mgk} - c_{gk}^{SU} - c_{gk}^{SD} \right) \quad (12)$$

s.t: (7) and equations (16)–(26) in [38].

$$Z^M = \min \sum_{k \in \mathcal{K}} \left(\sum_{a \in \mathcal{A}} C_a^R y_{ak}^R - \sum_{d \in \mathcal{D}} C_{dk}^D y_{dk}^D + \sum_{a \in \mathcal{A}} \left(\hat{\lambda}_{ak}^{i,P} z_{ak}^P + \hat{\lambda}_{ak}^{i,F+} z_{ak}^{F+} + \hat{\lambda}_{ak}^{i,F-} z_{ak}^{F-} + \hat{\lambda}_{ak}^{i,S+} z_{ak}^{S+} \right) \right) + \alpha + \sum_{c \in \mathcal{C}'} \hat{\lambda}_c^{i,C} (\beta_c - \alpha) \quad (13)$$

s.t: (8a)–(8c) and (8e)–(8l).

The market problem in (13) is solved as an LP problem which is coupled in time due to the HVDC ramping constraints in (8c). Power generation and reserve procurement in (8a)–(8g) are represented by the copy variables z_{ak}^P , z_{ak}^{F+} , z_{ak}^{F-} and z_{ak}^{S+} .

Unlike the work in [33], we avoid variable splitting on the reservoir variable when relaxing the Benders cuts in (8d). Instead, we let the hydropower subproblem in (11) and the market problem in (13) compute the different parts of (8d) that was relaxed. The set of cuts \mathcal{C} originally obtained from the long-term model can be reduced a priori according to the elimination procedure outlined in [39] (Section 4.3). As input to this procedure we compute the extremal reservoir boundaries at the end of the day, based on the maximum variation around the initial storage during the day, which depends on the values of the natural inflows and the discharge limits of the neighborhood plants in the same cascade. After the elimination, one is left with a reduced set of cuts \mathcal{C}' , where typically $|\mathcal{C}'| \ll |\mathcal{H}|$, and thus a relaxation procedure that is computationally efficient for systems with a large number of reservoirs. Note that the choice of long-term model will impact the magnitude of $|\mathcal{C}'|$ and possibly also the potential for cut elimination to arrive at $|\mathcal{C}'|$. In the case presented in Section V, using the long-term model in [3], we experienced that $|\mathcal{C}'|/|\mathcal{H}| < 0.01$.

A total of $4|\mathcal{A}||\mathcal{K}| + |\mathcal{C}'|$ Lagrangian multipliers need to be found, one for each energy and reserve product per price area and time step, and one for each Benders cut in the reduced set \mathcal{C}' .

B. Solving the Dual Problem

The dual problem in (14) consists of maximizing the Lagrangian dual function (15) with respect to the Lagrangian multipliers λ .

$$\max_{\lambda} \phi(\lambda) \quad (14)$$

$$\phi(\lambda) = \min_x \mathcal{L}(x, \lambda) \quad (15)$$

Problem (14) is nondifferentiable and concave, and its subgradients with respect to the Lagrangian multipliers can be found as the estimated mismatches in (9a)–(9d). We refer to these mismatches as g^i , where i is the iteration counter. The separable dual problem is solved as a quadratic programming (QP) program in (16) using the Bundle method [40]. The Bundle method is known for its stability, robustness and good convergence properties, as compared to other solving approaches for non-differentiable optimization, such as subgradient or standard cutting plane methods [31].

$$\max_{z, \lambda} z - \frac{1}{2\mu^k} \|\lambda - \hat{\lambda}^k\|^2 \quad (16a)$$

$$\text{s.t. : } z \leq \sigma^i + (g^i)^\top (\lambda - \hat{\lambda}^i), \quad i = 1 \dots k \quad (16b)$$

$$\sum_{c \in \mathcal{C}'} \lambda_c^C \leq 1 \quad (16c)$$

In (16) k denotes the current iteration, σ^i is the objective value of the primal problem in iteration i , μ^k is a penalty parameter, $\|\cdot\|$ is the 2-norm, and $\hat{\lambda}^k$ is the stable set of multipliers from a previous iteration. The guidelines for dynamically updating μ^k and $\hat{\lambda}^k$ follows the recommendations in [40]. Computed prices λ^k from (16) are declared new stability centers only when they provide a sufficient ascent for ϕ :

$$\phi(\lambda^k) \geq \phi(\hat{\lambda}^k) + m\delta, \quad (17)$$

where m is a parameter so that $0 \leq m \leq 1$, and $\delta = z^k - \phi(\hat{\lambda}^k)$ is the predicted increase. Regarding the stopping criterion, it depends on the norm of the so called “regularized subgradient,” computed at the current dual solution and considering the linearization error on the computation of the subgradients. More specifically, in each iteration k we compute $G = \frac{\lambda^k - \hat{\lambda}^k}{\mu^k}$ and a tolerance $\epsilon = \delta^k - \mu^k \|G\|^2$, according to [31], and stop when both $\epsilon \leq \text{tol}_\epsilon$ and $\|G\| \leq \text{tol}_G$.

Although several Benders cuts of type (8d) can be binding at the same time, the sum of their multipliers cannot exceed one. This inequality can be derived as a constraint in the dual formulation of the problem expressed in Section III, and is expressed in (16c). It ensures an efficient search for λ^C .

C. Solution Procedure

The LR solution procedure is illustrated in Fig. 4. In a given iteration i and for a set of multipliers $\hat{\lambda}^i$, the local hydro and thermal problems as well as the market problem are solved in a distributed environment. The optimal generation and reserve procurement solutions x_a^i are sent from the subproblems, and

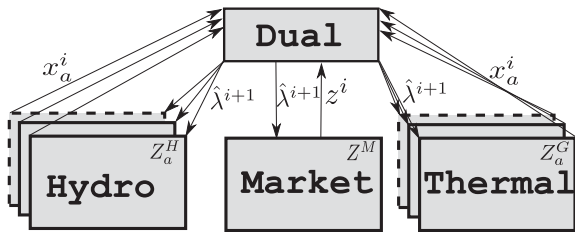


Fig. 4. LR solution procedure.



Fig. 5. Case study price areas and grid topology.

the copy variable solutions z^i from the market problem. Subsequently, the mismatches are computed in (9a)–(9d), and a new cut of type (16b) is added to the dual problem. After solving the dual problem (16), a new set of Lagrangian multipliers $\hat{\lambda}^{i+1}$ are found and sent back to the subproblems and the market problem.

We note that further improvements of the original Bundle method of [40] could be applied to solve the dual problem, as presented for example in [41], [42].

V. CASE STUDY

A. Case Description

We tested the model formulations on data description of the Northern European power system, with the price areas and grid topology illustrated in Fig. 5. The description reflects a scenario for the year 2030 with high levels of wind and solar power installed throughout Europe, as elaborated in [43]. Note that darker blue color in Fig. 5 reflects the countries represented by a higher level of detail in the data description. A detailed representation of the Nordic hydropower system is included, comprising 1093 hydropower modules, many of which are part of complex

hydropower cascades. To limit the number of binary variables, only the 549 modules with more than 10 MW installed capacity were represented with a binary status variable. We assumed their minimum production to be at 50% of the best efficiency point, and a 20% reduction in efficiency when operating at minimum production (point A in Fig. 3) compared to the best efficiency. A total of 252 thermal units are represented with start-up costs, minimum up- and down-times, and ramping constraints.

A spinning (up and down) and non-spinning (up) reserve requirement of 3000 MW and 4000 MW, correspondingly, was shared between Norway and Sweden. We assumed that 10% of the line capacities can be used for exchange of reserve capacity between the two countries' price areas, that only hydropower stations with more than 50 MW installed capacity are allowed to deliver spinning reserves, and that all power plants can deliver non-spinning reserves.

In order to cover a range of different system states and hydrological conditions, we selected 12 representative days by combining 4 different times of year (winter, spring, summer, autumn) and 3 different inflow years (wet, medium and dry). First, the long-term model was run to generate cuts of type (8d). The long-term model covered a time horizon of 3 years considering 58 different scenarios of inflow and wind power. Along each scenario and for each week in the long-term horizon, a two-stage stochastic LP was solved using Benders decomposition, as described in [3]. This solution process normally converges in 10-15 iterations, providing one Benders cut for each iteration. The long-term model was run on the same data set as the proposed short-term model. The minimum time resolution in the long-term model was 3 hours (gradually increasing along the horizon). A total of 781 of the hydropower modules have a reservoir capacity exceeding 2 Mm³, which was set as the lower limit to be a part of the end-of-horizon valuation provided by the Benders cuts. Finally, we applied the algorithm in [39] to reduce the number of Benders cuts prior to solving the short-term optimization problems, leaving us with a reduced set of typically 3-5 cuts.

The long-term model provided the initial reservoir volumes for the short-term model, and also suggested whether hydropower and thermal generators should initially be running or not. Note that the long-term model is based on (stochastic) LP and did not consider start-up costs and minimum generation levels. As a heuristic we assumed that stations and units that were initially running in the long-term model for the considered day were initially turned on in the short-term model.

In the presented short-term model, each day was run with hourly time resolution. We solved the same problem 3 times, first as an MIP problem following the formulation in Section III, then relaxing all integer variables using the LIR method and finally using LR method outlined in Section IV.

The model was implemented in Julia, using the JuMP package [44] and CPLEX 12.7 solver for solving the MIP, LP and QP problems. Both the full MIP and the MIP subproblems were solved with a relative MIP gap of 10⁻⁷. All optimization problems were run on server node with 2 10-core Intel Xeon E5-2640 processors with 2.50 GHz and 128 GB RAM.

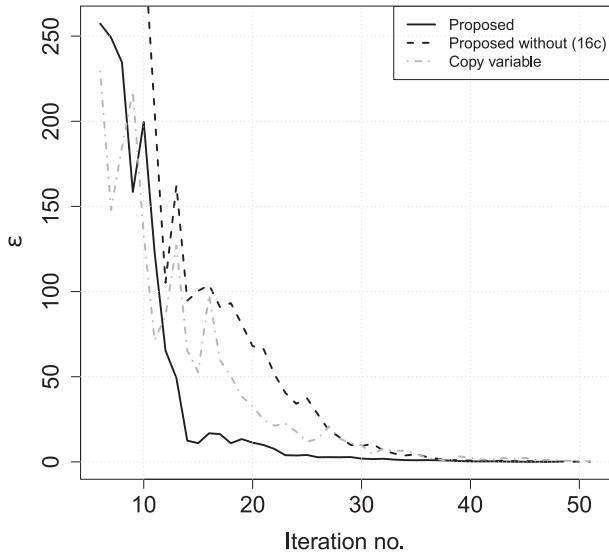


Fig. 6. Convergence for the LR solution process.

TABLE II
MIP OBJECTIVE FUNCTION VALUE (IN 10^6 €) AND COST GAPS BETWEEN
MIP-LIR AND MIP-LR (IN 10^3 €)

		Winter	Spring	Summer	Autumn
Dry	MIP	5790	4411	4614	4723
	MIP-LIR	1900	1402	2772	1948
	MIP-LR	525	424	736	680
Normal	MIP	5278	4036	4333	4141
	MIP-LIR	682	469	912	542
	MIP-LR	166	154	176	184
Wet	MIP	4212	3652	3720	4052
	MIP-LIR	372	359	530	278
	MIP-LR	112	124	158	126

B. Results

The full optimization problem did on average contain 670 thousand variables (19 thousand binary) and 420 thousand constraints. Solving these as full MIP and LIR problems took on average 2100 and 190 seconds, respectively. In comparison the average computation time for one LR iteration run with parallel processing on the 20-core server was 16 seconds, with convergence between 50-100 iterations. We applied a stopping criteria of $tol_\epsilon = tol_G = 10^{-3}$. Fig. 6 shows the convergence process (measured by ϵ) obtained for the Winter day using the proposed LR approach presented in Section IV. Convergence was achieved in 48 iterations. The figure also shows the convergence process when omitting (16c), as a black stapled line, converging in 74 iterations. Finally, we also tested the technique of duplicating variables per reservoir to relax Benders cuts in (8d), as described in [33]. This approach is shown with the grey stapled line in Fig. 6 and converged in 62 iterations. Similar convergence patterns were observed for the other representative days.

In line with theory, the operational costs obtained when solving the full MIP problem were always highest, followed by costs obtained by LR and then LIR. Table II shows the differences in costs between the MIP solution and the LIR and LR methods.

TABLE III
COST GAPS BETWEEN MIP-LIR AND MIP-LR CONSIDERING DIFFERENT
CHANGES ALL NUMBERS ARE IN 10^3 €

		Winter	Spring	Summer	Autumn
Base	MIP-LIR	682	469	912	542
	MIP-LR	166	154	176	184
HLP	MIP-LIR	98	108	102	94
	MIP-LR	36	39	36	32
TLP	MIP-LIR	670	440	846	453
	MIP-LR	156	136	154	118
InitDown	MIP-LIR	1438	963	1044	633
	MIP-LR	434	296	356	202
PQ-scale	MIP-LIR	550	412	660	498
	MIP-LR	148	146	114	163
NoDisRamp	MIP-LIR	622	480	922	480
	MIP-LR	160	139	250	171

The MIP objective function value is provided as a reference. The cost gaps between the three methods are significant, and the difference between LR and LIR indicates the potential in further tightening the LP problem solved in the latter. The MIP-LIR cost gap is highest for the summer day (when the system load is at its lowest) with dry weather conditions (high water values). Under such circumstances, hydropower stations are forced to run on a low output to meet the requirements for spinning reserve capacity and minimum river flows, typically operating in the non-concave part of the PQ-curve (point A illustrated in Fig. 3). We also observe that the gaps between the MIP solution and the two convex relaxations has significant dependence on the inflow year, being higher with less inflow.

In the two examples presented in Section II we illustrated the importance of involving the relaxed binary variables to obtain tight LP formulations. By introducing variable u_g when bounding generation per cost segment in (2b) and when limiting ramping in (4), the LP problem was tightened so that the LIR and LR solutions coincided for the two examples in Section II. Similarly, the use of the hydro unit commitment variable u_{hk} in the STHTS problem formulated in Section III serves to tighten the discharge ramping constraint (6f) and the segmented discharge (6i). To test the importance of this tightening, we solved the LIR LP problems for all cases reported in Table II without using u_{hk} in (6f) and (6i). The exclusion of u_{hk} in (6f) and (6i) contributed to an increased average MIP-LIR gap of 8.000 € and 114.000 €, respectively.

Next, we tested the sensitivities in the cost gaps obtained for the Normal inflow year in Table II to different changes in the model formulation and setup. The results are shown in Table III, where the type of change is indicated in the first column, and is explained in the following. The **Base** case is simply the reference with no changes; **HLP** relaxes the hydro unit commitment variable so that $u_{hk} \in [0, 1]$; **TLP** relaxes the thermal unit commitment variable so that $u_{gk} \in [0, 1]$; **InitDown** assumes that all thermal units that the long-term model dispatched below their minimum generation limits when entering the representative day in question were initially shut down in the STHTS model; **PQ-Scale** assumes no reduction in efficiency when operating at the minimum production (i.e. the PQ-curve follows points 0-B-C-D in Fig. 3 and point A is at best efficiency); and finally **NoDisRamp** relaxes limits on discharge ramping in (6f).

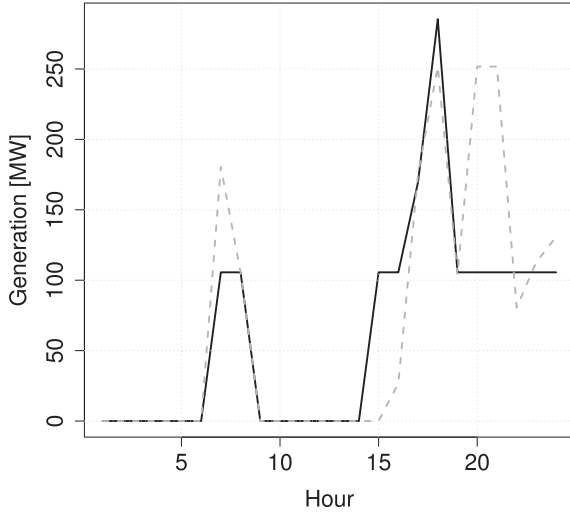


Fig. 7. Generation for a hydropower station obtained by the MIP (black) and LIR (stapled grey) approaches.

Note that each change shown in Table III was done separately. If we apply both the HLP and TLP changes, all binary variables are relaxed and the cost gaps are zero. We observe that the HLP change on average reduces the gaps to 15% (MIP-LIR) and 22% (MIP-LR) of their original values. For the TLP change the gaps are on average reduced to 92% (MIP-LIR) and 83% (MIP-LR) of their original values. The substantial differences between the average cost gap changes for the HLP and TLP changes should be seen in conjunction with the results from the InitDown change, where the latter indicates a strong dependency of the cost gaps on the initial state of thermal units. Applying the InitDown change increases the gaps with 57% (MIP-LIR) and 89% (MIP-LR). With the PQ-scale change the cost gaps are reduced to 81% (MIP-LIR) and 84% (MIP-LR). Finally, we observe that the NoDisRamp contributes to both decreasing and increasing the cost gaps.

Fig. 7 shows the generation schedule obtained by the MIP and LIR approaches for a specific hydropower station in Northern Sweden for the Normal Summer day. We observe that the MIP schedule always respects the minimum generation limit of 105 MW while the LIR schedule does not.

The MCE for the Normal Winter, Spring, Summer and Autumn days for a price area representing the western coast of Norway are shown in Figs. 8(a), 8(b), 8(c) and 8(d), respectively. The LIR and LR MCE follow each other closely, while prices from the MIP method deviates significantly in some peak hours. As discussed in Section II the LIR and LR MCE include the fixed cost elements while the MIP MCE does not, giving rise to deviations between LIR/LR and MIP MCE when decisions involving significant fixed costs are made. Similar patterns are found in Figs. 1 and 2. Moreover, we observe a tendency of the LR and MIP prices to be closer than LIR and MIP prices. This is most pronounced for the Autumn day in Fig. 8(d). A similar pattern was seen in Section II in Figs. 1 and 2, and can be explained by the fact that the LIR approach underestimates the convex cost envelope.

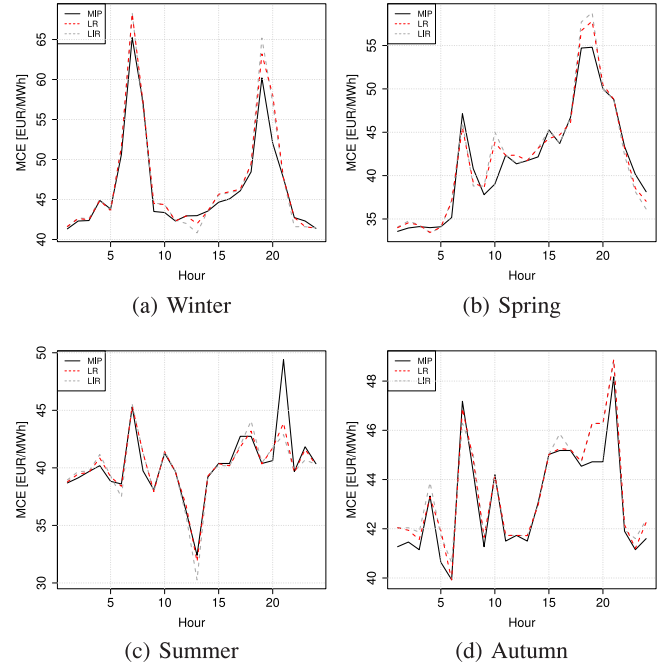


Fig. 8. MCE for western Norway for the Normal Winter, Spring, Summer and Autumn day.

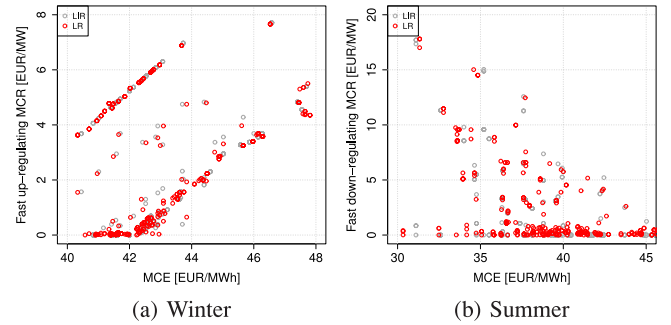


Fig. 9. Fast up-regulating MCR (winter) and down-regulating MCR (summer) vs MCE for all areas in Norway and Sweden.

Figs. 9(a) and 9(b) are scatter plots of fast up- and down-regulating MCR against MCE obtained for all Norwegian and Swedish price areas for a Normal Winter and Normal Summer day, respectively. The system is particularly challenged to provide fast up-regulation reserves during winter due to high demand. As expected, there is a clear positive correlation between fast up-regulating MCR and MCE in Fig. 9(a). For the Summer day there is sufficient up-regulation capacity, but some hydropower stations are kept running to meet the requirement for down-regulation reserves, and thus the negative correlation between down-regulating MCR and MCE in Fig. 9(b). Again, the LIR and LR prices do not differ significantly.

VI. CONCLUSION

In this work, we have compared two convex relaxations (LIR and LR) of the STHTS problem for data instances of the Northern European power system. In the formulation of the LR

algorithm, we focused on limiting the number of Lagrangian multipliers to facilitate computational efficiency.

In terms of operational costs, the LR method was in the range 55–81% closer than the LIR method to the MIP solution. Approximation errors for both the LIR and LR approach showed a clear seasonal variation, being highest for the representative summer day. Moreover, the MIP-LR cost gap was found to be less dependent on the hydrological conditions than the MIP-LIR gap. This gap difference indicates that one should be careful when forecasting operational costs in hydro-dominated systems with pronounced nonconvexities using the LIR approach. Although the LR approach closes much of the MIP-LIR cost gap, the MIP approach must be recommended for accurate cost estimates, provided that the computation time can be afforded.

We found that, for a given initial state of the system, the MIP-LIR and MIP-LR cost gaps could primarily be explained by the nonconvex representation of the hydropower system. In particular, the strict enforcement of the minimum power requirement for committed hydropower stations explained a substantial part of the gaps. On the other hand, the magnitude of the cost gaps substantially depended on the initial state of thermal generators, which underlines the importance of sound treatment of the commitment status of thermal units as state variables in the coupling between long- and short-term models.

Generally, the LR-LIR differences define the potential for further tightening the LP problem solved in the LIR method. This potential, which was significant in our case study, is worthwhile exploring through further research.

Regarding the marginal costs of electricity and reserve capacity (MCE and MCR), the results did not reveal significant differences between LIR and LR methods. Therefore, using the computationally tractable LIR method for MCE and MCR forecasting stands out like a reasonable choice.

VI. ACKNOWLEDGMENT

The authors would like to thank Dr. Bruno Fanzeres and the anonymous reviewers for their useful comments to this work.

REFERENCES

- [1] A. Haugstad and O. Rismark, "Price forecasting in an open electricity market based on system simulation," in *Proc. Int. Conf. Elect. Power Syst. Oper. Manage.*, Zürich, Switzerland, 1998.
- [2] C. Weber, "Uncertainty in the electric power industry: Methods and models for decision support," 1st ed., *ser. Int. Ser. Operations Res. Manage. Sci.* Springer, 2004.
- [3] A. Helseth, B. Mo, A. L. Henden, and G. Warland, "Detailed long-term hydro-thermal scheduling for expansion planning in the nordic power system," *IET Gener., Transmiss. Distrib.*, vol. 12, no. 2, pp. 441–447, 2018.
- [4] M. Maceira *et al.*, "Twenty years of application of stochastic dual dynamic programming in official and agent studies in brazil - main features and improvements on the NEWAVE model," in *Proc. 20th Power Syst. Comput. Conf.*, 2018.
- [5] J. Kong, H. I. Skjelbred, and O. B. Fosso, "An overview on formulations and optimization methods for the unit-based short-term hydro scheduling problem," *Electric Power Syst. Res.*, vol. 178, 2020.
- [6] A. L. Diniz, T. Santos, R. Cabral, L. Santos, M. E. Maceira, and F. Costa, "Short/Mid-term hydrothermal dispatch and spot pricing for large-scale systems - the case of brazil," in *Proc. 20th Power Syst. Comput. Conf.*, 2018.
- [7] A. Brigatto, A. Street, and D. M. Valladão, "Assessing the cost of time-inconsistent operation policies in hydrothermal power systems," *IEEE Trans. Power Syst.*, vol. 32, no. 6, pp. 4914–4923, Nov. 2017.
- [8] P. Gribik, W. Hogan, and S. Pope, "Market-clearing electricity prices and energy uplift, harvard electricity policy group working," Paper, Dec. 2007.
- [9] M. VanVyve, "Linear prices for non-convex electricity markets: Models and algorithms," Center for operations research and econometrics, discussion Paper 2011/50, 2011.
- [10] G. Wang, U. V. Shanbhag, T. Zheng, E. Litvinov, and S. Meyn, "An extreme-point subdifferential method for convex hull pricing in energy and reserve markets-Part i: Algorithm structure," *IEEE Trans. Power Syst.*, vol. 28, no. 3, pp. 2111–2120, Aug. 2013.
- [11] D. A. Schiro, T. Zheng, F. Zhao, and E. Litvinov, "Convex hull pricing in electricity markets: Formulation, analysis, and implementation challenges," *IEEE Trans. Power Syst.*, vol. 31, no. 5, pp. 4068–4075, Sep. 2016.
- [12] B. Hua and R. Baldick, "A convex primal formulation for convex hull pricing," *IEEE Trans. Power Syst.*, vol. 32, no. 5, pp. 3814–3823, Sep. 2017.
- [13] H. Chao, "Incentives for efficient pricing mechanism in markets with non-convexities," *J. Regulatory Econ.*, vol. 56, pp. 33–58, 2019.
- [14] Z. Yang, T. Zheng, J. Yu, and K. Xie, "A unified approach to pricing under nonconvexity," *IEEE Trans. Power Syst.*, vol. 34, no. 5, pp. 3417–3427, Sep. 2019.
- [15] Y. Yu, Y. Guan, and Y. Chen, "An extended integral unit commitment formulation and an iterative algorithm for convex Hull pricing," *IEEE Trans. Power Syst.*, vol. 35, no. 6, pp. 4335–4346, Nov. 2020.
- [16] R. Hytowitz and E. Ela, "Current practice and research gaps in alternative (fast-start) price formation modeling," Electric power research institute (EPRI), independent system operator and regional transmission organization price formation working group White Paper 3002013724, 2019.
- [17] B. Kneueven, J. Ostrowski, A. Castillo, and J. Watson, "Computationally efficient algorithm for computing convex hull prices," 2020 [Online]. Available: <http://www.optimization-online.org/>
- [18] B. Kneueven, J. Ostrowski, and J. Watson, "On mixed-integer programming formulations for the unit commitment problem," *Inform. J. Comput.*, 2020.
- [19] C. Gentile, G. Morales-España, and A. Ramos, "A tight MIP formulation of the unit commitment problem with start-up and shut-down constraints," *EURO J. Comput. Optim.*, vol. 5, pp. 177–201, 2017.
- [20] B. Hua, B. Huang, R. Baldick, and Y. Chen, "Tight formulation of transition ramping of combined cycle units," *IEEE Trans. Power Syst.*, vol. 35, no. 3, pp. 2167–2175, 2020.
- [21] W. van Ackooij, I. D. Lopez, A. Frangioni, F. Lacalandra, and M. Tahanan, "Large-scale unit commitment under uncertainty: An updated literature survey," *Ann. Oper. Res.*, vol. 271, pp. 11–85, 2018.
- [22] A. Diniz and M. E. P. Maceira, "A four-dimensional model of hydro generation for the short-term hydrothermal dispatch problem considering head and spillage effects," *IEEE Trans. Power Syst.*, vol. 23, no. 3, pp. 1298–1308, 2008.
- [23] S. Cerisola, J. M. Latorre, and A. Ramos, "Stochastic dual dynamic programming applied to nonconvex hydrothermal models," *Eur. J. Oper. Res.*, vol. 218, pp. 687–697, 2012.
- [24] G. Steeger and S. Rebennack, "Dynamic convexification within nested benders decomposition using Lagrangian relaxation: An application to the strategic bidding problem," *Eur. J. Oper. Res.*, vol. 257, no. 2, pp. 669–686, 2017.
- [25] M. N. Hjelmeland, J. Zou, A. Helseth, and S. Ahmed, "Nonconvex medium-term hydropower scheduling by stochastic dual dynamic integer programming," *IEEE Trans. Sustain. Energy*, vol. 10, no. 1, pp. 481–490, Jan. 2018.
- [26] E. Pereira-Bonvallet, S. Püschel-Lovengreen, M. Matus, and R. Moreno, "Optimizing hydrothermal scheduling with non-convex irrigation constraints," *Energy Procedia*, vol. 87, pp. 132–150, 2016. [Online]. Available: <https://www.sciencedirect.com/journal/energy-procedia/vol/87/suppl/C>
- [27] A. L. Diniz and T. M. Souza, "Short-term hydrothermal dispatch with river-level and routing constraints," *IEEE Trans. Power Syst.*, vol. 29, no. 5, pp. 2427–2435, Sep. 2014.
- [28] A. Borghetti, A. Frangioni, F. Lacalandra, and C. A. Nucci, "Lagrangian heuristics based on disaggregated bundle methods for hydrothermal unit commitment," *IEEE Trans. Power Syst.*, vol. 18, no. 1, pp. 313–323, Feb. 2003.
- [29] C. Lemaréchal, C. Sagastizábal, F. Pellegrino, and A. Renaud, "Bundle methods applied to the unit-commitment problem," in *System Modelling and Optimization*, Boston, MA, USA: Springer, pp. 395–402, 1996.

- [30] E. Ni, X. Guan, and R. Li, "Scheduling hydrothermal power systems with cascaded and head-dependent reservoirs," *IEEE Trans. Power Syst.*, vol. 14, no. 3, pp. 1127–1132, Aug. 1999.
- [31] A. Belloni, A. L. Diniz, M. E. P. Maceira, and C. A. Sagastizábal, "Bundle relaxation and primal recovery in unit commitment problems. The Brazilian case," *Ann. Operations Res.*, vol. 120, pp. 21–44, 2003.
- [32] A. L. Diniz, C. Sagastizábal, and M. E. P. Maceira, "Assessment of lagrangian relaxation with variable splitting for hydrothermal scheduling," in *Proc. IEEE Power Eng. Soc. General Meeting*, Tampa, FL, 2007, pp. 1–8.
- [33] F. Y. K. Takigawa, E. L. daSilva, E. C. Finardi, and R. N. Rodrigues, "Solving the hydrothermal scheduling problem considering network constraints," *Electric Power Syst. Res.*, vol. 88, pp. 89–97, 2012.
- [34] M. R. Scuzziato, E. C. Finardi, and A. Frangioni, "Comparing spatial and scenario decomposition for stochastic hydrothermal unit commitment problems," *IEEE Trans. Sustain. Energy*, vol. 9, no. 3, pp. 1307–1317, Jul. 2018.
- [35] I. Herrero, P. Rodilla, and C. Batlle, "Electricity market-clearing prices and investment incentives: The role of pricing rules," *Energy Econ.*, vol. 47, pp. 42–51, 2015.
- [36] C. Vazquez, M. Hallack, and M. Vazquez, "Price computation in electricity auctions with complex rules: An analysis of investment signals," *Energy Policy*, vol. 105, pp. 550–561, 2017.
- [37] P. Damci-Kurt, S. Küçükayavuz, D. Rajan, and A. Atamtürk, "A polyhedral study of production ramping," *Math. Program., Ser.*, vol. 158, pp. 175–205, 2016.
- [38] M. Carrión and J. M. Arroyo, "A computationally efficient mixed-integer linear formulation for the thermal unit commitment problem," *IEEE Trans. Power Syst.*, vol. 21, no. 3, pp. 1371–1378, Aug. 2006.
- [39] A. Shapiro, W. Tekaya, M. P. Soares, and J. Paulo daCosta, "Worst-case-expectation approach to optimization under uncertainty," *Oper. Res.*, vol. 61, no. 6, pp. 1435–1449, 2013.
- [40] C. Lemaráchal and C. Sagastizábal, "Variable metric bundle methods: From conceptual to implementable forms," *Math. Program.*, vol. 76, no. 3, pp. 393–410, 1997.
- [41] G. Emiel and C. Sagastizábal, "Incremental-like bundle methods with application to energy planning," *Comput. Optim. Appl.*, vol. 46, pp. 305–322, 2010.
- [42] W. van Ackooij and W. de Oliveira, "Level bundle methods for constrained convex optimization with various oracles," *Comput. Optim. Appl.*, vol. 57, pp. 555–597, 2014.
- [43] L. E. Schaeffer, B. Mo, and I. Graabak, "Electricity prices and value of flexible generation in northern Europe in 2030," in *Proc. 13th Int. Conf. Eur. Energy Market*, 2019.
- [44] I. Dunning, J. Huchette, and M. Lubin, "JuMP: A modeling language for mathematical optimization," *SIAM Rev.*, vol. 59, no. 2, pp. 295–320, 2017.

Arild Helseth (Member, IEEE) received his M.Sc. and Ph.D. degrees in electrical power engineering from the Norwegian University of Science and Technology (NTNU), in 2003 and 2008, respectively. Currently, he is a Senior Research Scientist at SINTEF Energy Research, where he has been employed since 2008. His research experience includes mathematical modeling and optimization algorithms applied to electricity markets and power systems, particularly within the field of generation scheduling in hydro-dominated systems.

Stefan Jaehnert received his Dipl.-Ing. within electrical and mechanical engineering from the Chemnitz University of Technology (Germany), in 2007. He received the Ph.D. degree within the field of power markets and power systems from the Norwegian University of Science and Technology (NTNU) in 2012. Since 2012, he has been with SINTEF Energy Research. His research experience is within modeling and techno-economic analyses of power markets and power systems. The main research is on hydro-thermal power system and the integration of renewable energy sources with a focus on short-term system balancing as well as the long-term adequacy development of power systems.

André Luiz Diniz (Senior Member, IEEE) received the B.Sc. degree in civil engineering in 1996, the M.Sc. degree in operations research in 2000, and the D.Sc. degree in optimization in 2007, from the Federal University of Rio de Janeiro (UFRJ), Rio de Janeiro, Brazil. Since 1998, he has been a Researcher with CEPEL, the Brazilian Electric Energy Research Center, working in the development of optimization models for power generation planning and also as a Project Manager. Since 2017, he is the Head of the Optimization and Environment Department (DEA) of CEPEL. He is also an Assistant Professor with the Institute of Mathematics and Statistics, State University of Rio de Janeiro (UERJ), where he teaches courses on probability, statistics and decision making. He has substantial experience in several subjects related to optimization, such as linear, dynamic and stochastic programming, as well as application of decomposition methods to large scale problems in the power industry.